



UPPSALA  
UNIVERSITET

# Data-driven modeling of avascular tumors

---

Fredrik Gustafsson, Fredrik Jonasson, Oscar Larsson

**Project in Computational Science: Report**

February 2020

PROJECT REPORT



## Abstract

In this report we start with a short review of the history of mathematical models for tumor growth. We then look at three specific models for avascular tumor growth, tumor growth with deformable ECM [1], the effects of external pressure on tumor growth [2], and the effects of cell-cell and cell-matrix adhesion [3]. We use the finite element method to solve the partial differential equations implemented in FEniCS. However due to implementation problems we are only able to produce results from two of the models, after simplifying them. The results show that without any adhesive directed growth [3] yields a symmetric tumor with growing radius and with a fixed tumor size [2] eventually runs out of nutrients and the mass fraction of necrotic tumor cells increases.

# Contents

<b>1</b>	<b>Introduction</b>	<b>1</b>
<b>2</b>	<b>A Brief History of Tumor Modeling</b>	<b>1</b>
<b>3</b>	<b>Tumor Models</b>	<b>3</b>
3.1	Model 1 (Sciunmè) . . . . .	3
3.2	Model 2 (Chaplain) . . . . .	6
3.3	Model 3 (Mascheroni) . . . . .	7
<b>4</b>	<b>FEniCS</b>	<b>10</b>
<b>5</b>	<b>Results</b>	<b>11</b>
5.1	Sciunmè . . . . .	11
5.2	Chaplain . . . . .	11
5.3	Mascheroni . . . . .	12
<b>6</b>	<b>Discussion</b>	<b>13</b>

# 1 Introduction

Since the mid 20th century scientists have become more aware of the difficulties of treating cancer [2, 4, 5], and that it requires cooperation between different fields to successfully find new cures [6]. Based on work done by Greenspan et al. in 1976 [7], mathematical models describing the basic progression of tumors could be made. Most continuum models, as the three models investigated herein, focus on the avascular phase [2], which is the state of a tumor before they have developed their own blood vessels supplying nutrition.

Continuum models for tumor growth are of a reaction-diffusion character including tumor cells, matrix degrading enzymes, the extracellular matrix, and concentrations of cell substrates e.g. oxygen and inhibitors [8]. More recent work has also included different ways for locomotion such as diffusion, haptotaxis or internal pressure. Researchers have also developed models in order to investigate the relation between the micro environment, e.g. available nutrients or mechanical stress-factors, and tumor growth. Models investigating the behaviour of the tumor movements influenced by cell-cell adhesion [9] and cell-matrix adhesion [10] have also been constructed.

Another way to model tumors, compared to reaction-diffusion models, is by treating the system as a porous solid. One such model ([11],[12]) defines the extracellular matrix as a solid while the tumors, living and necrotic, and interstitial fluids are seen as fluids. Such models are referred to as multiphase flow models and can be useful when studying cancer by considering mass transportation within the tumor [13].

This project aims at implementing three models, one continuum model [3] and two multiphase models ([1],[2]), using the finite element method and the FEniCS library, to validate the implementation by comparing the results with published results.

## 2 A Brief History of Tumor Modeling

One early model of tumor growth was presented by A.K. Laird in 1964 [4]. There, a model for tumor size as a function of time was derived from experimental data, fitted to a so called Gompertz equation. Laird found that the growth of tumors initially started as exponential but deviated more and more from this, due to retardation, as time increased giving it a non-constant growth rate, compared to a simple exponential function. Following this model, the growth would reach an asymptote placing a limit on the growth of the tumor. Furthermore the author argued that the retardation was due to an increase in mean generation time during the growth. This was in contrast with the statements of Mayneord who, in 1932, had shown that the retardation could be explained by the tumors having a necrotic core, decreasing the region of active growth [5].

Findings in 1972 by Sutherland and Durand [14] found that tumors could stop growing without the development of a necrotic core. A model, incorporating the findings of [14], was proposed by D.L.S McElwain and L.E. Morris in 1978 [15]. Their model assumed that the growth would be affected not only by the formation of a necrotic core but also by apoptosis, i.e. programmed cell death. Other work on the steady state limit was performed by Folkman and Hochberg [16]. They found that the nutrients eventually are not enough for the tumor to continue growing and the core of the tumor will start dying. A steady state will arise, where tumor growth at the border will offset the death at the center of the tumor. The model proposed by Folkman and Hochberg deals with three-dimensional tumor growth, while applying a differing amount of stress to the tumor to see how it affects the growth. Some earlier works, where similar experiments were performed, are the 1971 paper by Sutherland et al. [17], and later on with the inclusion of mechanical stress, by Helmlinger et al. [18] and Kaufman et al. [19]. Early continuum models of spherical tumor growth focus primarily on the nutrition diffusion and the biochemical processes [20]. A later paper by Chaplain et al. in 2006 [21] was among the earliest to reflect these experiments on the effects of external stress on cell proliferation into their mathematical models.

Further studies on the role of the necrotic core and nutrients and their effect on tumor growth were performed by Greenspan who published a paper in 1976 [7]. In his model, the growth and motion of the tumor was due to internal pressure due to birth and death of cells. From his experiments he came to the conclusion that as the tumor grows it can reach an unsteady state in which it might split or disintegrate. He argued that The latter could start a sequence of growth and division thereby overcoming the steady state limit.

While Greenspan focused on the role of nutrients and the necrotic core Glass [22] focused on chemical inhibitors, in a paper published in 1973 [22]. Glass discussed a simple one dimensional model incorporating growth inhibitors, so called chalcones, a model which he claimed was motivated due to evidence surrounding cellular growth being controlled by negative feedback from the tissue. The model assumed uniform production of the growth inhibitors and that the growth was regulated by a switch mechanism, i.e. if the concentration of chalcones was below the threshold, growth would occur. The work by Glass was expanded in the 80s by John Adam in a series of three papers [23, 24, 25]. In the first paper, published in 1986 [23], he found that the growth was sensitive to non-uniform source terms for the inhibitors. The second paper [24], published in 1987, focused not only on a non-uniform source term but also on different three-dimensional geometries, e.g. thin rod, thin disk, and sphere. As in the case of non-uniform source term he argued that the geometry of the source also affected the growth of tumors. The third paper [25], published in 1989, in cooperation with S.A. Maggelakis, compared two mathematical models. These two models deviated from those studied in Adam's previous papers by modelling the inhibitors as a product of other processes. The first model focused on modelling the inhibition as a product of necrosis while the second model instead assumed that the inhibitors were a product of living cells metabolic processes.

One of the earliest spatial models for tumor growth was presented in 1996 by Robert A. Gatenby and Edward T. Gawlinski [26]. They proposed a model based of previous work done by Gatenby [27, 28]. Rather than fitting data to a Gompertz equation this model was based upon modelling the tumor-host interaction using population ecology models with limited resources. Furthermore, they considered changes in the surrounding tissues due to released acids, resulting in an environment unsuitable for healthy cells, while tumor cells survives and proliferates. The model itself consisted of three coupled reaction-diffusion equations for healthy tissue, tumors and acid.

The effect of haptotaxis on the dynamics between the healthy tissue, tumors and degrading enzymes was further investigated [29]. In 2000 A.R.A Anderson et al. [30] presented their work on investigating this dynamic. Their continuum model did not include any cell proliferation. Instead focusing solely upon the haptotactic effects. They also extended the model to two dimensions as well as developing a discrete version of their model.

Anderson continued to investigate the haptotactic dynamic for tumor cell motion and published a paper in 2005 [31], where the model was extended to include an equation for the available oxygen. In the paper Anderson investigates the effect of oxygen and the effect of cell-cell adhesion by using a hybrid discrete-continuum model and modelled the adhesion as a value which dictated how many neighbours a cell needed in order to be allowed to migrate.

Another approach for modelling the cell-cell and cell-tissue adhesion was presented in 2008 by A. Gerisch and M.A.J. Chaplain [32]. Their model was based upon the one presented in 2000 by Anderson but included a non-local cell-cell and cell-tissue adhesion term instead of the previous local haptotactic term, resulting in a continuum model with directed growth from adhesion.

Sciumè et al. presented a new model in 2013 [33]. They derived the governing equations for their model through thermodynamically constrained averaging theory (TCAT) framework presented by [34]. TCAT was used to go from microscopic laws to macroscale relationships in order to extend multiphase porous media mechanics to tumor models. In a subsequent paper published in 2013, Sciumè et al. [12] further developed the model by introducing constitutive relationship between pressure differences. What they found was that the tension in the interface between the different phases led to different growth patterns for the tumor.

### 3 Tumor Models

In this section three models for tumor growth are presented. The first paper [1] models tumors at the macroscopic scale using TCAT to translate relations on the microscopic scale to macroscopic. The tumors are represented by a multiphase flow model. The second paper, [3], uses a reaction-diffusion equation with a non-local adhesion directed growth term. The third and last model, [2], is an extension to [1] and incorporates the influence of external pressure on tumor growth.

#### 3.1 Model 1 (Sciumè)

The tumor growth model by Sciumè [1, 11] consists of three mass balance governing equations for the tumor cell, the host cell and the interstitial fluid. In the mass balance equations, there are different phases which include the tumor cell, the host cell, the extracellular matrix (ECM) and the interstitial fluid. The ECM, the area around the cells and what gives them structure, constitutes the solid phase while tumor cell, host cell and interstitial fluids constitute the liquid phases. The governing equations describes the behaviour of the differential pressures, where  $u(1)$  is the differential pressure between the tumor and host cell,  $u(2)$  is the differential pressure between the host cell and the interstitial fluids, and  $u(3)$  is the pressure in the interstitial fluids.

In the following equations, (1)-(3),  $\varepsilon$  denotes the porosity of the ECM from which the volume fraction occupied by the solid phase can be calculated as  $\varepsilon^s = 1 - \varepsilon$ ,  $S$  is the saturation degree of the different fluid phases, tumor cells, host cells, and interstitial fluids, for phase  $x$  the saturation degree is defined as  $S^x = \varepsilon^x / \varepsilon$  volume fraction divided by porosity. In this model there are three fluid phases and  $S^t + S^h + S^l = 1$ . The relation between the three saturation degrees are as follows,  $S^l = 1 - [\frac{2}{\pi} \arctan(\frac{u(2)}{a})]$  and  $S^h + S^l = S^t = 1 - [\frac{2}{\pi} \arctan(\frac{\sigma_{hl}}{\sigma_{th}} \frac{u(1)}{a})]$ , where  $\sigma_{ij}$  is the interfacial tension between phase  $i$  and phase  $j$  while  $a$  is a constant related to  $\varepsilon$ .

The three mass balance equations for the tumor cell are as follows:

$$\begin{aligned}
 & \left[ \frac{\varepsilon S^t}{K_T} + \frac{S^t(1-\varepsilon)}{K_S} \left( S^t + u(1)S_{der}^t \right) + \varepsilon S_{der}^t \right] \frac{\partial u(1)}{\partial t} \\
 & + \left[ \frac{\varepsilon S^t}{K_T} + \frac{S^t(1-\varepsilon)}{K_S} \left( 1 - S^l - u(2)S_{der}^l \right) \right] \frac{\partial u(2)}{\partial t} \\
 & + \left[ \frac{\varepsilon S^t}{K_T} + \frac{S^t(1-\varepsilon)}{K_S} \right] \frac{\partial u(3)}{\partial t} \\
 & = \nabla \cdot \left[ \frac{k_{rel}^t \mathbf{k}}{\mu^t} \cdot \nabla \left( u(1) + u(2) + u(3) \right) \right] \\
 & - S^t \left( \mathbf{1} : \mathbf{d}^s \right) - \nabla S^t \cdot \left( \varepsilon \mathbf{v}^s \right) + \frac{1}{\rho^t} M^{l \rightarrow t},
 \end{aligned} \tag{1}$$

for the host cell,

$$\begin{aligned}
& \left[ \frac{S^h(1-\varepsilon)}{K_S} \left( S^t + u(1)S_{der}^t \right) - \varepsilon S_{der}^t \right] \frac{\partial u(1)}{\partial t} \\
& + \left[ \frac{\varepsilon S^h}{K_H} + \frac{S^h(1-\varepsilon)}{K_S} \left( 1 - S^l - u(2)S_{der}^l \right) - \varepsilon S_{der}^l \right] \frac{\partial u(2)}{\partial t} \\
& + \left[ \frac{\varepsilon S^h}{K_H} + \frac{S^h(1-\varepsilon)}{K_S} \right] \frac{\partial u(3)}{\partial t} \\
& = \nabla \cdot \left[ \frac{k_{rel}^h \mathbf{k}}{\mu^h} \cdot \nabla \left( u(2) + u(3) \right) \right] \\
& - S^h \left( \mathbf{1} : \mathbf{d}^s \right) - \nabla S^h \cdot \left( \varepsilon \mathbf{v}^s \right),
\end{aligned} \tag{2}$$

for the interstitial fluid,

$$\begin{aligned}
& \left[ \frac{\varepsilon S^t}{K_T} + \frac{1-\varepsilon}{K_S} \left( S^t + u(1)S_{der}^t \right) \right] \frac{\partial u(1)}{\partial t} \\
& + \left[ \frac{\varepsilon S^t}{K_T} + \frac{\varepsilon S^h}{K_H} + \frac{1-\varepsilon}{K_S} \left( 1 - S^l - u(2)S_{der}^l \right) \right] \frac{\partial u(2)}{\partial t} \\
& + \left( \frac{\varepsilon S^t}{K_T} + \frac{\varepsilon S^h}{K_H} + \frac{\varepsilon S^l}{K_L} + \frac{1-\varepsilon}{K_S} \right) \frac{\partial u(3)}{\partial t} \\
& = \nabla \cdot \left[ \frac{k_{rel}^t * \mathbf{k}}{\mu^t} \cdot \nabla u(1) \right] \\
& + \nabla \cdot \left[ \left( \frac{k_{rel}^t * \mathbf{k}}{\mu^t} + \frac{k_{rel}^h * \mathbf{k}}{\mu^h} \right) \cdot \nabla u(2) \right] \\
& + \nabla \cdot \left[ \left( \frac{k_{rel}^t * \mathbf{k}}{\mu^t} + \frac{k_{rel}^h * \mathbf{k}}{\mu^h} + \frac{k_{rel}^l * \mathbf{k}}{\mu^l} \right) \cdot \nabla u(3) \right] \\
& - S^t \left( \mathbf{1} : \mathbf{d}^s \right) + \frac{\rho^l - \rho^t}{\rho^t \rho^l} M^{l \rightarrow t}.
\end{aligned} \tag{3}$$

As mentioned in [1],  $K_x$  is the compressibility of phase x,  $\mu^x$  is the dynamic viscosity of phase x,  $k_{rel}^x$  is the relative permeability for phase x  $\mathbf{k}$  the intrinsic permeability tensor of the ECM,  $\mathbf{d}^s$  is the Eulerian rate of strain tensor,  $\mathbf{v}^s$  is the velocity of the solid phase,  $\rho^x$  is the density of phase x and  $M^{l \rightarrow t}$  is an inter-phase exchange of mass between the interstitial fluid phase and the phase of the tumor cell. ":" denotes the double dot product, in this case between the rate of strain tensor and the identity matrix.

To solve (1)-(3) numerically, the finite element method is used. The test space  $V$  is defined by  $V = \{v : \|\nabla v\| + \|v\| < \infty\}$ , then the equations (1)-(3) are multiplied by  $v_1$ ,  $v_2$  and  $v_3$  respectively, where  $v_1, v_2, v_3 \in V$ .

After the multiplication with the test functions we partially integrate each function and get the following three equations

$$\begin{aligned}
& \int_{\Omega} \left[ \frac{\varepsilon S^t}{K_T} + \frac{S^t(1-\varepsilon)}{K_S} \left( S^t + u(1)S_{der}^t \right) + \varepsilon S_{der}^t \right] \frac{\partial u(1)}{\partial t} v_1 dx \\
& + \int_{\Omega} \left[ \frac{\varepsilon S^t}{K_T} + \frac{S^t(1-\varepsilon)}{K_S} \left( 1 - S^l - u(2)S_{der}^l \right) \right] \frac{\partial u(2)}{\partial t} v_1 dx \\
& + \int_{\Omega} \left[ \frac{\varepsilon S^t}{K_T} + \frac{S^t(1-\varepsilon)}{K_S} \right] \frac{\partial u(3)}{\partial t} v_1 dx \\
& = - \int_{\Omega} \left[ \frac{k_{rel}^t \mathbf{k}}{\mu^t} \cdot \nabla \left( u(1) + u(2) + u(3) \right) \right] \cdot \nabla v_1 dx \\
& \quad - \int_{\Omega} S^t \left( \mathbf{1} : \mathbf{d}^s \right) v_1 dx + \int_{\Omega} S^t \cdot \left( \varepsilon \mathbf{v}^s \right) \nabla v_1 dx + \int_{\Omega} \frac{1}{\rho^t} M^{l \rightarrow t} v_1 dx,
\end{aligned} \tag{4}$$

$\forall v_1 \in V$ , where the right hand side can be simplified using integration by parts.

The weak form for (2) becomes

$$\begin{aligned}
& \int_{\Omega} \left[ \frac{S^h(1-\varepsilon)}{K_S} \left( S^t + u(1)S_{der}^t \right) - \varepsilon S_{der}^t \right] \frac{\partial u(1)}{\partial t} v_2 dx \\
& + \int_{\Omega} \left[ \frac{\varepsilon S^h}{K_H} + \frac{S^h(1-\varepsilon)}{K_S} \left( 1 - S^l - u(2)S_{der}^l \right) - \varepsilon S_{der}^l \right] \frac{\partial u(2)}{\partial t} v_2 dx \\
& + \int_{\Omega} \left[ \frac{\varepsilon S^h}{K_H} + \frac{S^h(1-\varepsilon)}{K_S} \right] \frac{\partial u(3)}{\partial t} v_2 dx \\
& = \int_{\Omega} \left[ \frac{k_{rel}^h \mathbf{k}}{\mu^h} \cdot \nabla \left( u(2) + u(3) \right) \right] \cdot \nabla v_2 dx \\
& \quad - \int_{\Omega} S^h \left( \mathbf{1} : \mathbf{d}^s \right) v_2 dx + \int_{\Omega} S^h \cdot \left( \varepsilon \mathbf{v}^s \right) \cdot \nabla v_2 dx,
\end{aligned} \tag{5}$$

$\forall v_2 \in V$ , where the right hand side can be simplified using integration by parts.

and for (3) the weak form becomes

$$\begin{aligned}
& \int_{\Omega} \left[ \frac{\varepsilon S^t}{K_T} + \frac{1-\varepsilon}{K_S} \left( S^t + u(1)S_{der}^t \right) \right] \frac{\partial u(1)}{\partial t} v_3 dx \\
& + \int_{\Omega} \left[ \frac{\varepsilon S^t}{K_T} + \frac{\varepsilon S^h}{K_H} + \frac{1-\varepsilon}{K_S} \left( 1 - S^l - u(2)S_{der}^l \right) \right] \frac{\partial u(2)}{\partial t} v_3 dx \\
& + \int_{\Omega} \left( \frac{\varepsilon S^t}{K_T} + \frac{\varepsilon S^h}{K_H} + \frac{\varepsilon S^l}{K_L} + \frac{1-\varepsilon}{K_S} \right) \frac{\partial u(3)}{\partial t} v_3 dx \\
& = - \int_{\Omega} \left[ \frac{k_{rel}^t * \mathbf{k}}{\mu^t} \cdot \nabla u(1) \right] \cdot \nabla v_3 dx \\
& \quad - \int_{\Omega} \left[ \left( \frac{k_{rel}^t * \mathbf{k}}{\mu^t} + \frac{k_{rel}^h * \mathbf{k}}{\mu^h} \right) \cdot \nabla u(2) \right] \cdot \nabla v_3 dx \\
& \quad - \int_{\Omega} \left[ \left( \frac{k_{rel}^t * \mathbf{k}}{\mu^t} + \frac{k_{rel}^h * \mathbf{k}}{\mu^h} + \frac{k_{rel}^l * \mathbf{k}}{\mu^l} \right) \cdot \nabla u(3) \right] \cdot \nabla v_3 dx \\
& \quad - \int_{\Omega} S^t \left( \mathbf{1} : \mathbf{d}^s \right) v_3 dx + \int_{\Omega} \frac{\rho^l - \rho^t}{\rho^t \rho^l} M^{l \rightarrow t} v_3 dx,
\end{aligned} \tag{6}$$

$\forall v_3 \in V$ , where the right hand side can be simplified using integration by parts.

To discretise the system (4)-(6) in time we use the Euler backward method with timestep  $\Delta t$ , i.e.  $\frac{\partial u(x)}{\partial t}$  is replaced by  $\frac{u(x)_h^{n+1} - u(x)_h^n}{\Delta t}$  and every other occurrence of  $u(x)$  is replaced by  $u(x)_h^{n+1}$  where  $x = 1, 2, 3$ .



### 3.2 Model 2 (Chaplain)

Following the non-local model presented by Chaplain in 2008 [32] and further investigated by Chaplain in 2014 [3] the governing equations for tumor growth, for one population, are

$$\frac{\partial c}{\partial t} = \nabla \cdot (D_1 \nabla c - cA(t, \chi, \mathbf{u}(t, \cdot))) + P(t, \mathbf{u})c, \quad (7)$$

$$\frac{\partial v}{\partial t} = -\gamma m v + \psi(t, \mathbf{u}), \quad (8)$$

$$\frac{\partial m}{\partial t} = \nabla \cdot (D_3 \nabla m) + \alpha c - \lambda m, \quad (9)$$

in which  $c$  is the tumor cell concentration,  $v$  is the extracellular matrix density and  $m$  is the concentration of matrix degrading enzymes (MDE). Equation (7)-(9) introduce the constants  $D_1$  which is the random motility coefficient of the tumor population,  $\gamma$  corresponds to the rate constant of the degradation of ECM due to MDE,  $D_3$  is the diffusion constant of the MDE, the secretion rate of MDE from the tumor population is modelled by  $\alpha$ , and finally  $\lambda$  is the decay constant for the MDE. Furthermore,  $\mathbf{u}(t, \chi) = (c(t, \chi)^T, v(t, \chi))^T$  which is the combined cell concentration and ECM density vector,  $\psi(t, \mathbf{u})$  is the remodelling of the ECM,  $\chi = [x_1 \ x_2]^T$  which is the spatial dimension vector, and  $P(t, \mathbf{u})$  is the tumor cell proliferation. The non-local operator  $A(t, \chi, \mathbf{u}(t, \cdot))$  representing the velocity of directed cell migration from cell-cell and cell-matrix adhesion and is defined as

$$A(t, \chi, \mathbf{u}(t, \cdot)) = \frac{1}{R} \int_{B(0, R)} n(y) \cdot \Omega(\|y\|_2) g(t, \mathbf{u}(t, x+y)) dy, \quad (10)$$

where  $n(y)$  is the unit vector between point  $x$  and  $x+y$  and  $\Omega(\|y\|_2) = \frac{3}{\pi R^2} (1 - \frac{\sqrt{x^2+y^2}}{R})$  is a distance dependency function. Finally the term  $g(t, \mathbf{u}(t, x+y))$  is defined as  $g(t, \mathbf{u}(t, x+y)) = (S_{cc}c + S_{cv}v) * (1 - d_v v - d_c c)^+$  where  $S_{cc}$  and  $S_{cv}$  are the cell-cell and cell-matrix adhesion coefficients, the  $+$  sign in the second term is the positive part, i.e.,  $\max(0, \cdot)$ , of the inhibition of migration from volume filling effects,  $d_v v$  and  $d_c c$  are the fractions of the physical space occupied by  $v$  and  $c$  respectively. In this case we chose

$$P(t, \mathbf{u}) = \mu_1 (1 - d_v v - d_c c), \quad (11)$$

which yields a logistic growth with competition for space for the tumor cells. For the three equations (7)-(9) the following two boundary conditions hold, for  $t \in I_T$  and  $\chi \in D$

$$(D_1 \nabla c - cA(t, \chi, \mathbf{u}(t, \cdot))) \cdot n(\chi) = 0, \quad t \in I_T, \chi \in \partial D, \quad (12)$$

$$(\nabla m) \cdot n(\chi) = 0, \quad t \in I_T, \chi \in \partial D, \quad (13)$$

where  $n(\chi)$  is the normal vector on  $\partial D$ ,  $I_T$  is the time domain and  $D$  is the spatial domain. Finally the initial conditions are as follows,  $c_0(\chi)$ ,  $v_0(\chi)$  and  $m_0(\chi)$ , for numerical values see [3].

To solve the equations, (7)-(9), we will use a finite element method. First we define a test space  $V$ ,  $V = \{v : \|\nabla v\| + \|v\| < \infty\}$ , we then multiply the equations, (7)-(9) with test functions,  $v_1$ ,  $v_2$  and  $v_3$  respectively, where  $v_1, v_2, v_3 \in V$ . After the multiplication with the test functions we partially integrate each function and obtain the following three equations:

$$\frac{\partial c}{\partial t} = \int_D (-(D_1 \nabla c - cA(t, \chi, \mathbf{u}(t, \cdot))) \cdot \nabla v_1 + P(t, \mathbf{u})c v_1) d\chi, \quad \forall v_1 \in V \quad (14)$$

$$\frac{\partial v}{\partial t} = \int_D (-\gamma m v v_2 + \psi(t, \mathbf{u})v_2) d\chi, \quad \forall v_2 \in V \quad (15)$$

$$\frac{\partial m}{\partial t} = \int_D (-(D_3 \nabla m) \cdot v \nabla v_3 + \alpha c v_3 - \lambda m v_3) d\chi, \quad \forall v_3 \in V. \quad (16)$$

To form a variational form we add the three equations together

$$\begin{aligned} & \frac{\partial c}{\partial t} + \int_D ((D_1 \nabla c - c A(t, \chi, \mathbf{u}(t, \cdot))) \cdot \nabla v_1 - P(t, \mathbf{u}) c v_1) d\chi \\ & + \frac{\partial v}{\partial t} + \int_D (\gamma m v v_2 - \psi(t, \mathbf{u}) v_2) d\chi, \quad \forall v_1, v_2, v_3 \in V \quad (17) \\ & + \frac{\partial m}{\partial t} + \int_D ((D_3 \nabla m) \cdot v \nabla v_3 - \alpha c v_3 + \lambda m v_3) d\chi = 0. \end{aligned}$$

Next we let  $K = \{\mathcal{K}\}$  be a mesh consisting of regular triangles,  $\mathcal{K}$ , of  $D$  and define  $V_h \subset V$  as the space of all continuous piecewise linear functions on  $K$  that fulfill the boundary conditions (12)-(13). This results in the system

$$\begin{aligned} & \frac{\partial c_h}{\partial t} + \int_D ((D_1 \nabla c_h - c_h A(t, \chi, \mathbf{u}_h(t, \cdot))) \cdot \nabla v_1 - P(t, \mathbf{u}_h) c_h v_1) d\chi \\ & + \frac{\partial v_h}{\partial t} + \int_D (\gamma m_h v_h v_2 - \psi(t, \mathbf{u}_h) v_2) d\chi, \quad \forall v_1, v_2, v_3 \in V \quad (18) \\ & + \frac{\partial m_h}{\partial t} + \int_D ((D_3 \nabla m_h) \cdot v \nabla v_3 - \alpha c_h v_3 + \lambda m_h v_3) d\chi = 0. \end{aligned}$$

where  $c_h, v_h, m_h \in V_h$ . Finally we discretise the time derivatives in (18) using the backward Euler method with timestep  $\Delta t$ . This leads to the final space and time discretised system

$$\begin{aligned} & \frac{c_h^{n+1} - c_h^n}{\Delta t} v_1 + \int_D ((D_1 \nabla c_h^{n+1} - c_h^{n+1} A(t, \chi, \mathbf{u}_h^{n+1}(t, \cdot))) \cdot \nabla v_1 - P(t, \mathbf{u}_h^{n+1}) c_h^{n+1} v_1) d\chi \\ & + \frac{v_h^{n+1} - v_h^n}{\Delta t} v_2 + \int_D (\gamma m_h^{n+1} v_h^{n+1} v_2 - \psi(t, \mathbf{u}_h^{n+1}) v_2) d\chi, \quad \forall v_1, v_2, v_3 \in V \quad (19) \\ & + \frac{m_h^{n+1} - m_h^n}{\Delta t} + \int_D ((D_3 \nabla m_h^{n+1}) \cdot v \nabla v_3 - \alpha c_h^{n+1} v_3 + \lambda m_h^{n+1} v_3) d\chi = 0. \end{aligned}$$

The non-local term is calculated by solving the integral around each node in the two spatial directions separately by letting the unit normal work in one direction, i.e. each node has two values  $A_x$  and  $A_y$ .

### 3.3 Model 3 (Mascheroni)

The third tumor growth model investigated in this work is presented by Mascheroni et. al in 2016, [2]. The model includes a term for describing any external pressure applied to the tumor cells during growth, either applied by the surrounding fluid or a mechanical compression of the cells. This model has three governing equations, one for the tumor volume fraction  $\varepsilon^s$ , one for the mass fraction of necrotic tumor cells  $\omega^{Nt}$  and one for the mass fraction of the nutrition in the model, oxygen,  $\omega^{ox}$ . The three governing equations are as follows:

$$\frac{\partial \varepsilon^s}{\partial t} - \frac{1}{r^2} \frac{\partial}{\partial r} \left( r^2 \varepsilon^s \frac{k}{\mu^l} \Sigma' \frac{\partial \varepsilon^s}{\partial r} \right) - \frac{1}{\rho} \left( \overset{l \rightarrow s}{M} - \overset{s \rightarrow l}{M} \right) = 0, \quad (20)$$

$$\frac{\partial (\omega^{Nt} \varepsilon^s)}{\partial t} - \frac{1}{r^2} \frac{\partial}{\partial r} \left( r^2 \varepsilon^s \omega^{Nt} \frac{k}{\mu^l} \Sigma' \frac{\partial \varepsilon^s}{\partial r} \right) - \frac{1}{\rho} \left( \varepsilon^s r^{Nt} - \overset{s \rightarrow l}{M} \right) = 0, \quad (21)$$

$$\frac{\partial [(1 - \varepsilon^s) \omega^{ox}]}{\partial t} + \frac{1}{r^2} \frac{\partial}{\partial r} \left( r^2 \varepsilon^s \omega^{ox} \frac{k}{\mu^l} \Sigma' \frac{\partial \varepsilon^s}{\partial r} \right) - \frac{1}{r^2} \frac{\partial}{\partial r} \left[ r^2 (1 - \varepsilon^s) D^{ox} \frac{\partial \omega^{ox}}{\partial r} \right] + \frac{1}{\rho} \overset{ox \rightarrow s}{M} = 0, \quad (22)$$

with boundary conditions:

$$\frac{\partial \varepsilon^s}{\partial r} = \frac{\partial \omega^{Nt}}{\partial r} = \frac{\partial \omega^{ox}}{\partial r} = 0, \quad \text{in } r = 0, \quad (23)$$

$$\varepsilon^s = \varepsilon_{ext}^s, \quad \omega^{Nt} = 0, \quad \omega^{ox} = \omega_{env}^{ox}, \quad \text{in } r = R, \quad (24)$$

and initial conditions:

$$\varepsilon^s = \varepsilon_{ext}^s, \quad \omega^{Nt} = 0, \quad \omega^{ox} = \omega_{env}^{ox}, \quad \text{on } 0 < r < R \text{ at } t = 0. \quad (25)$$

As the tumor grows and expands, the outer boundary  $R$  should also move alongside the boundary conditions. The velocity of the outer boundary is defined as:

$$\frac{dR}{dt} = -\frac{k}{\mu^l} \Sigma' \frac{\partial \varepsilon^s}{\partial r}. \quad (26)$$

The equations are expressed in polar coordinates but due to spherical symmetry the equations only depend on the tumor radius  $r$  and can as such be reduced to a one-dimensional problem.

As for the parameters in the equations all three of the terms  $\overset{l \rightarrow s}{M}$ ,  $\overset{s \rightarrow l}{M}$  and  $\overset{ox \rightarrow s}{M}$  are mass transfer terms that describe the mass exchange between the three phases of the model, where  $l$  represents the interstitial fluid (IF),  $s$  is the solid phase consisting of tumor cells and the extracellular matrix, and  $ox$  is the nutrition, oxygen. The term  $k$  is the intrinsic permeability of the solid matrix and  $\mu^l$  is the dynamic viscosity which together form the hydraulic permeability  $k/\mu^l$ . The term  $\Sigma'$  is the derivative of  $\Sigma$  with respect to  $\varepsilon^s$  which is represented by a pseudo-potential law describing the force between two cells [35]. The densities of both the solid phase  $s$  and the fluid phase  $l$  are the same as they are assumed to be incompressible and are represented by  $\rho$  in the equations above. The rate of death of the living tumor cells (LTC) is represented by the term  $\varepsilon^s r^{Nt}$  and the term  $D^{ox}$  represents the diffusion coefficient of oxygen.

The expression for the pseudo-potential law is as follows:

$$\Sigma(\varepsilon^s) = \begin{cases} \alpha(\varepsilon^s - \varepsilon_0^s)^2 \left[ \frac{1 - \varepsilon_n^s}{(1 - \varepsilon^s)^\beta} - \frac{1}{(1 - \varepsilon_0^s)^\beta} \right], & \text{if } \varepsilon^s > \varepsilon_0^s \\ 0, & \text{otherwise,} \end{cases} \quad (27)$$

where  $\varepsilon_0^s$  and  $\varepsilon_n^s$  are defined as 1/3 and 0.8 respectively [35]. The rate of death term  $\varepsilon^s r^{Nt}$  has the following form:

$$\varepsilon^s r^{Nt} = \gamma_n^s I(\omega^{ox}) \omega^{Lt} \varepsilon^s. \quad (28)$$

The tumor phase  $s$  includes the sub-phases living tumor cells and necrotic tumor cells (NTC) and as the mass fractions of each phase sum to 1, the following holds:  $\omega^{Lt} = 1 - \omega^{Nt}$ . The rate of cell death is controlled by  $\gamma_n^s$ , while the function  $I$  describes cell death as a result of lack of oxygen.

The interphase mass exchange terms  $\overset{l \rightarrow s}{M}$ ,  $\overset{s \rightarrow l}{M}$  and  $\overset{ox \rightarrow s}{M}$  are defined as follows:

$$\overset{l \rightarrow s}{M} = \gamma_g^s G(\omega^{ox}) H(t_{eff}^s) \omega^{Lt} \varepsilon^s, \quad (29)$$

$$\overset{s \rightarrow l}{M} = \lambda_l^s \omega^{Nt} \varepsilon^s, \quad (30)$$

$$\overset{ox \rightarrow s}{M} = \gamma_0^s \frac{\omega^{ox}}{\omega^{ox} + c^{ox}} \omega^{Lt} \varepsilon^s. \quad (31)$$

The term accounting for the nutrient consumption of the tumor described in (31) is validated via experiments performed in 1992 by Casciari et al. [36] whereas the other two terms,  $\overset{l \rightarrow s}{M}$  and  $\overset{s \rightarrow l}{M}$  are described by Preziosi and Sciumè amongst others [37, 33]. The tumor phase  $s$  consists of the sub-phases living tumor cells and necrotic tumor cells and as the mass fractions of each phase sum to 1, the following holds:  $\omega^{Lt} = 1 - \omega^{Nt}$ . The effective stress tensor  $t_{eff}^s$  is defined as  $t_{eff}^s = -\Sigma(\varepsilon^s)\mathbf{I}$  as per [2]. The parameter  $\gamma_g^s$  describes the nutrient uptake due to cell growth that happens when the IF becomes tumor cells. The functions  $G$  and  $H$  describe effects of the nutrient level and growth inhibition due to mechanical stress respectively. Cell membrane degradation for the phase transition between  $s$  and  $l$  is described by  $\lambda_l^s$ . Finally the terms  $\gamma_0^s$  and  $\omega_{crit}^{ox}$  both describe oxygen uptake,  $\gamma_0^s$  the uptake order of magnitude, and  $\omega_{crit}^{ox}$  the level where oxygen consumption is halved. The three functions  $G$ ,  $H$  and  $I$  were selected from various earlier works [35, 38, 39, 40, 37, 41, 33]. The function  $H$  differs but the form was verified to better fit this model via experiments [2]. The functions  $G$ ,  $H$  and  $I$  have the forms:

$$G(\omega^{ox}) = \left\langle \frac{\omega^{ox} - \omega_{crit}^{ox}}{\omega_{env}^{ox} - \omega_{crit}^{ox}} \right\rangle_+, \quad (32)$$

$$H(t_{eff}^s) = 1 - \delta_1 \frac{\langle \Sigma \rangle_+}{\langle \Sigma \rangle_+ + \delta_2}, \quad (33)$$

$$I(\omega^{ox}) = \left\langle \frac{\omega_{crit}^{ox} - \omega^{ox}}{\omega_{env}^{ox} - \omega_{crit}^{ox}} \right\rangle_+, \quad (34)$$

where the angle brackets signify the positive value of the argument.

Similar to the other two models, the governing equations (20), (21) and (22) are implemented in FEniCS. To formulate the weak form of the governing equations we first determine which are the variables to solve for, either the mixed terms  $[\varepsilon^s, \omega^{Nt} \varepsilon^s, (1 - \varepsilon^s) \omega^{ox}]$  or to separate the terms and solve for  $[\varepsilon^s, \omega^{Nt}, \omega^{ox}]$ . Here the second option is chosen. Starting with equation (20), multiply by  $r^2$ , introducing a test function  $v_1$  and integrate over the domain.

$$\int_0^R r^2 \frac{\partial \varepsilon^s}{\partial t} v_1 dr - \int_0^R \frac{\partial}{\partial r} \left( r^2 \varepsilon^s \frac{k}{\mu^l} \Sigma' \frac{\partial \varepsilon^s}{\partial r} \right) v_1 dr - \int_0^R \frac{r^2}{\rho} \left( \overset{l \rightarrow s}{M} - \overset{s \rightarrow l}{M} \right) v_1 dr = 0. \quad (35)$$

Using Gauss' theorem yields:

$$\int_0^R r^2 \frac{\partial \varepsilon^s}{\partial t} v_1 dr - \int_0^R \frac{\partial}{\partial r} \left( r^2 \varepsilon^s \frac{k}{\mu^l} \Sigma' \frac{\partial \varepsilon^s}{\partial r} \right) v_1 dr \quad (36)$$

$$+ \int_0^R r^2 \varepsilon^s \frac{k}{\mu^l} \Sigma' \frac{\partial \varepsilon^s}{\partial r} \frac{\partial v_1}{\partial r} dr - \int_0^R \frac{r^2}{\rho} \left( \overset{l \rightarrow s}{M} - \overset{s \rightarrow l}{M} \right) v_1 dr = 0. \quad (37)$$

Applying the boundary conditions listed in (23) and (24) results in the second term being equal to zero, leaving as the final weak form of the first governing equation:

$$\int_0^R r^2 \frac{\partial \varepsilon^s}{\partial t} v_1 dr + \int_0^R r^2 \varepsilon^s \frac{k}{\mu^l} \Sigma' \frac{\partial \varepsilon^s}{\partial r} \frac{\partial v_1}{\partial r} dr - \int_0^R \frac{r^2}{\rho} \left( \overset{l \rightarrow s}{M} - \overset{s \rightarrow l}{M} \right) v_1 dr = 0. \quad (38)$$

Following the same procedure for the other two governing equations results in:

$$\int_0^R r^2 \frac{\partial(\omega^{Nt} \varepsilon^s)}{\partial t} v_2 dr + \int_0^R r^2 \varepsilon^s \omega^{Nt} \frac{k}{\mu^l} \Sigma' \frac{\partial \varepsilon^s}{\partial r} \frac{\partial v_2}{\partial r} dr - \int_0^R \frac{r^2}{\rho} \left( \varepsilon^s r^{Nt} - M \right) v_2 dr = 0, \quad (39)$$

$$\begin{aligned} & \int_0^R r^2 \frac{\partial[(1 - \varepsilon^s) \omega^{ox}]}{\partial t} v_3 dr - \int_0^R r^2 \varepsilon^s \omega^{ox} \frac{k}{\mu^l} \Sigma' \frac{\partial \varepsilon^s}{\partial r} \frac{\partial v_3}{\partial r} dr \\ & + \int_0^R r^2 (1 - \varepsilon^s) D^{ox} \frac{\partial \omega^{ox}}{\partial r} \frac{\partial v_3}{\partial r} dr + \int_0^R \frac{r^2}{\rho} M v_3 dr = 0. \end{aligned} \quad (40)$$

We discretize (38)-(40) using linear FEM and the Euler backward method to discretize in time. The resulting fully discretized system has the form:

$$\int_0^R r^2 \frac{\varepsilon_h^{s,n+1} - \varepsilon_h^{s,n}}{\Delta t} v_{h,1} dr + \int_0^R r^2 \varepsilon_h^{s,n+1} \frac{k}{\mu^l} \Sigma' \frac{\partial \varepsilon_h^{s,n+1}}{\partial r} \frac{\partial v_{h,1}}{\partial r} dr - \int_0^R \frac{r^2}{\rho} \left( M - M \right) v_{h,1} dr = 0, \quad (41)$$

$$\begin{aligned} & \int_0^R r^2 \left( \frac{\omega_h^{Nt,n+1} - \omega_h^{Nt,n}}{\Delta t} \varepsilon_h^{s,n+1} + \frac{\varepsilon_h^{s,n+1} - \varepsilon_h^{s,n}}{\Delta t} \omega_h^{Nt,n+1} \right) v_{h,2} dr \\ & + \int_0^R r^2 \varepsilon_h^{s,n+1} \omega_h^{Nt,n+1} \frac{k}{\mu^l} \Sigma' \frac{\partial \varepsilon_h^{s,n+1}}{\partial r} \frac{\partial v_{h,2}}{\partial r} dr - \int_0^R \frac{r^2}{\rho} \left( \varepsilon_h^{s,n+1} r^{Nt} - M \right) v_{h,2} dr = 0, \end{aligned} \quad (42)$$

$$\begin{aligned} & \int_0^R r^2 \left( [1 - \varepsilon_h^{s,n+1}] \frac{\omega_h^{ox,n+1} - \omega_h^{ox,n}}{\Delta t} - \frac{\varepsilon_h^{s,n+1} - \varepsilon_h^{s,n}}{\Delta t} \omega_h^{ox,n+1} \right) v_{h,3} dr \\ & - \int_0^R r^2 \varepsilon_h^{s,n+1} \omega_h^{ox,n+1} \frac{k}{\mu^l} \Sigma' \frac{\partial \varepsilon_h^{s,n+1}}{\partial r} \frac{\partial v_{h,3}}{\partial r} dr + \int_0^R r^2 (1 - \varepsilon_h^{s,n+1}) D^{ox} \frac{\partial \omega_h^{ox,n+1}}{\partial r} \frac{\partial v_{h,3}}{\partial r} dr \\ & + \int_0^R \frac{r^2}{\rho} M v_{h,3} dr = 0. \end{aligned} \quad (43)$$

## 4 FEniCS

FEniCS is a software library for solving PDEs using finite element methods [42]. It consists of a number of components such as DOLFIN, FFC, FIAT, Instant, mshr and UFL working together.

FFC, which stands for FEniCS form compiler, is the part which provides a compiler for automatic evaluation of variational problems [43]. By using FFC as the form compiler one can express

problems with the *Unified Form Language* or UFL. UFL can be used to express finite element problems "in a near mathematical way" [44] which generates an abstract representation of the problem which can then be interpreted using FFC. To generate the basis functions the component finite element automatic tabulator or FIAT is used [45]. UFC, Unified Form-assembly Code, works together with the other components and are used to assemble the matrices and vectors which FEM gives rise to [46]. The software, written in C++, which brings the previously mentioned software components together is DOLFIN [47]. DOLFIN allows the user to specify a finite element problem in a variational form using UFL and FFC which is then evaluated using basis functions generated by FIAT on a mesh constructed with mshr. Furthermore DOLFIN has a Python interface and C++ interface to allow programming to be done in either language.

## 5 Results

None of three models investigated were implemented completely, and as such the results shown are not complete either. The second model (Chaplain) is missing the adhesion directed growth term, and the third model (Mascheroni) lacks the moving boundary and is as such only simulated for a fixed radius.

### 5.1 Sciumè

For the model by Sciumè [1] the velocity terms for the solid phase was not described in a way that made the model reproducible. The treatment of the solid phase, the ECM, is the main focus and new for this model, but in the article the terms that are used and the implementation for the calculated results were not explained in a clear enough way for us to be able to reproduce and implement this model.

### 5.2 Chaplain

When running the simulation the following values suggested by Chaplain et al. [3] was used:  $D_1 = 10^{-4}$ ,  $\mu_1 = 0.1$ ,  $\gamma = 10$ ,  $D_3 = 10^{-3}$ ,  $\alpha = 0.1$ ,  $\lambda = 0.5$ ,  $R = 0.1$ ,  $S_{cc} = 0.5$  and  $S_{cv} = 0.1$ . As in the original paper no remodeling of the ECM takes place i.e.  $\psi(t, \mathbf{u}) = 0$ . A change compared to the model in [3] is that  $S_{cc}$  changes abruptly from its initial value to  $S_{cc} = 0.48$ .

The results of solving (19) from  $t = 0$  to  $t = 0.05$  using FEniCS are shown below in Figure 1.

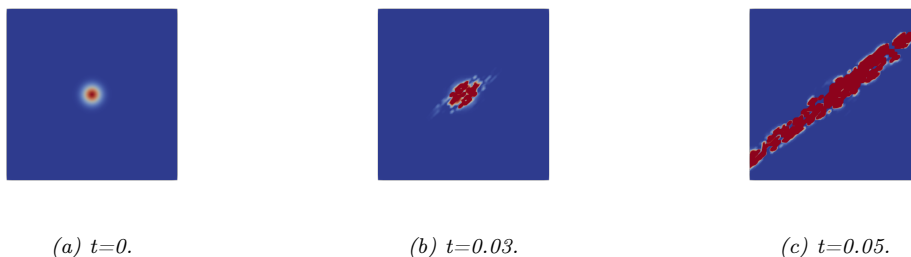


Figure 1: Solution to (19) for the concentration of tumor cells,  $c$ , at time 0, 0.03 and 0.05 when setting  $\psi(t, \mathbf{u}) = 0$ .

The results of setting  $A(t, \chi, \mathbf{u}(t, \cdot)) = 0$ , no adhesion guided directed cell migration, and solving the system from  $t = 0$  to  $t = 60$  using are shown below in Figure 2.

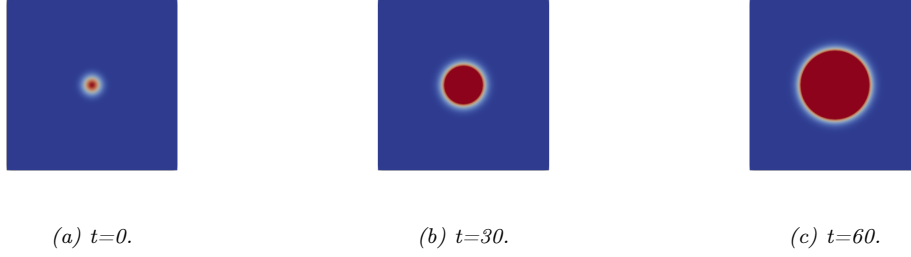


Figure 2: Solution to (19) for the concentration of tumor cells,  $c$ , at time 0, 30 and 60 when setting  $\psi(t, \mathbf{u})$  and  $A(t, \chi, \mathbf{u}(t, \cdot)) = 0$ .

### 5.3 Mascheroni

After deriving the discrete system of equations (41)-(43), to implement it in FEniCS, first we define the discretization mesh. For this model, the symmetry reduces the problem to 1D, and as such a 1D mesh can be used. Next, we define the test- and trial functions by defining a mixed element as the product space of the three basis functions  $v_1, v_2, v_3$  and use that to define the function space to be able to represent the entire system as a single entity. Each of the basis functions are defined as class P1 according to the Periodic Table of the Finite Elements. Define the boundary and initial conditions listed in equations (23), (24) and (25) on the appropriate subspaces. To solve the mixed equation system where the variables are present in multiple of the governing equations, add all of the equations together and set the right hand side to zero. This is done to combine all of the equations into one FEniCS-object and to be able to use the built-in Newton solver for nonlinear problems, as the equations are nonlinear. To handle the tumor growing, the boundary conditions presented in (23) and (24) has to be moved along with the outer boundary of the tumor moving. The boundary moves with velocity according to (26). To implement this in FEniCS, two different approaches were tried. The first was to create a new mesh between each timestep, slightly larger as the tumor will have grown, and then interpolate the solution onto the new mesh. The second approach was to use a large enough mesh from the start of the simulation, but to introduce a penalty method and then move where the penalty should be applied each timestep. Both of these approaches require that the velocity of the boundary can be evaluated numerically, either to define the new mesh endpoint, or to be able to move the penalty. This is where the implementation of this model got stuck as the expression was not able to be evaluated due to mismatching data and object types in Python and FEniCS.

The results presented below are for a simulation where the radius of the tumor is fixed at  $200\mu m$  with the parameter values used as  $\omega_{env}^{ox} = 7.0 \cdot 10^{-6}$ ,  $c_{ox} = 1.48 \cdot 10^{-7}$ ,  $\gamma_0^s = 3.0 \cdot 10^{-4} \text{ kg}/(\text{m}^3\text{s})$ ,  $\beta = 0.5$ ,  $\varepsilon_{ext}^s = 0.8$ ,  $\varepsilon_0^s = 1/3$ ,  $k = 1.8 \cdot 10^{-15} \text{ m}^2$ ,  $\mu^l = 1.0 \cdot 10^{-3} \text{ Pa s}$ ,  $D^{ox} = 3.2 \cdot 10^{-9} \text{ m}^2/\text{s}$ ,  $\rho = 1.0 \cdot 10^3 \text{ kg}/\text{m}^3$ ,  $\omega_{ox}^{crit} = 2.0 \cdot 10^{-6}$ ,  $\gamma_g^s = 5.4 \cdot 10^{-3} \text{ kg}/(\text{m}^3\text{s})$ ,  $\gamma_n^s = 1.5 \cdot 10^{-1} \text{ kg}/(\text{m}^3\text{s})$ ,  $\lambda_l^s = 1.15 \cdot 10^{-2} \text{ kg}/(\text{m}^3\text{s})$ , and  $\alpha = 1.0 \cdot 10^5 \text{ Pa}$ .

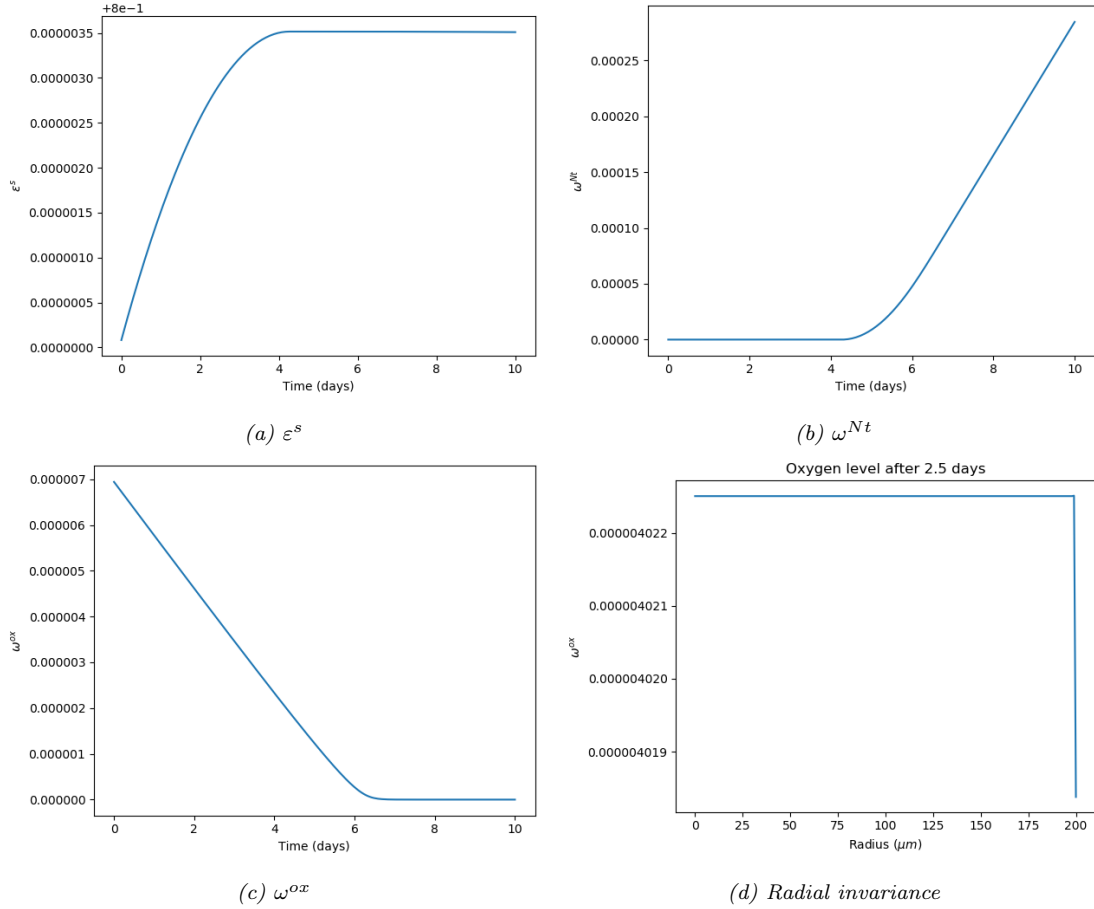


Figure 3: Solutions to the governing equations (20)-(22) while using a fixed radius  $R = 200\mu\text{m}$ .

As the expression for how much the boundary should move between timesteps could not be evaluated the boundary conditions of the model were not implemented correctly and as such, the model only runs for a fixed radius.

## 6 Discussion

Figure 2 shows that without any adhesion directed cell growth or ECM remodelling the solution to (19) behaves like a diffusion equation without a decreasing concentration within the tumor, i.e. the radius of the tumor increases giving it a symmetrical growth. When adding the adhesion directed term we get the results in Figure 1 where the tumor clearly have a directed growth. However the results are unrealistic since it not only grows into the shape of a band but also have discontinuous regions, regions not connected to the main population, and healthy regions surrounded by tumors. Furthermore the built in non-linear Newton solver in FEniCS fails to solve (19) after  $t = 0.05$ , within 1000 steps, when the same domain as in [3] is used. The domain size is claimed in [3] to be large enough such that the tumor should not grow to the limit of the domain. This problem might have to do with the tumor concentration reaching the limit of the computational domain, unit square centred around zero, and according to [3] the tumor should not reach said limit.

From these results, Figure 1 and Figure 2, one can draw two conclusions. First the tumor grows unrealistically fast when the adhesion directed growth term is added, the implementation of said non local integral is most likely incorrect. Second, without the adhesion directed growth term the tumor grows symmetrically and without any necrosis. Such growth is a naive and unrealistic



way of modelling a tumor since it does not react with the environment nor showcase any cell death, which could imply that the proliferation of the tumor cells are high enough to maintain a constant concentration of cells within the tumor, which once again seems unrealistic. Hence one can conclude that for a realistic tumor growth model a diffusion-reaction equation does not give a satisfying result, provided that the adhesion directed term was the only part not implemented correctly.

The results of the Mascheroni simulations shows in Figure 3a that the volume fraction of tumor cells  $\varepsilon^s$  approximately stays the same as the initial condition, with a slight increase before plateauing. Figure 3b shows that the mass fraction of necrotic tumor cells  $\omega^{Nt}$  increases and Figure 3c that the mass fraction of oxygen  $\omega^{ox}$  decreases as time passes. As the tumor does not expand and there is no flow of nutrition through the boundary of the tumor the tumor cells will die due to low levels of nutrition, which explains the increase in necrotic tumor cells. The volume fraction of tumor cells stays the same as the only changes happening to the solid phase is LTC becoming NTC, both which are a part of the solid phase, as such the total volume fraction is the same. Similarly the oxygen decreases due to the tumor cells consuming oxygen before starting to die as the oxygen is consumed. If the radius were to expand over time the tumor would have access to a supply of oxygen, meaning that the tumor could grow at the boundary, while dying in the center, creating a radial dependency which is not present in the simulations as shown by Figure 3d. The sharp dropoff at the outer boundary of the tumor is negligible as the error is of the order  $10^{-9}$ .

Evidently, the implementation for each model was unsuccessful, most likely due to a lack of knowledge regarding how to implement the models in FEniCS. The problem displayed in Figure 1 is most likely due to the non-local integral being implemented incorrectly while for the model presented in [2] we did not manage to implement a moving boundary. With more time these problems might have been solved by us getting more experience with FEniCS or trying to seek the help from more someone with more knowledge about implementing similar problems in FEniCS. Furthermore, more time would have allowed us to persue other ways to try and solve the problems, i.e. using trapezoidal rule for integrating the non-local operator instead of FEniCS built in integration. Had we however manage to implement the models correctly then one way to combine the models would be to use the continuum model of Chaplain [3] to compute how the boundary should move and then use this data in Mascheroni [2] model. However such a combination would not be trivial and would most likely mean that the spherical symmetry would be lost increasing the complexity of implementing the model. At the same time such a model would hopefully be able to describe the interplay between nutrients and adhesion for both growth and movement of tumors leading to a better invasion model.

## References

- [1] G Sciumè et al. “A tumor growth model with deformable ECM”. In: *Physical Biology* 11.6 (Nov. 2014), p. 065004.
- [2] Pietro Mascheroni et al. “Predicting the growth of glioblastoma multiforme spheroids using a multiphase porous media model”. In: *Biomechanics and Modeling in Mechanobiology* 15 (Jan. 2016), pp. 1215–1228.
- [3] Pia Domschke et al. “Mathematical modelling of cancer invasion: Implications of cell adhesion variability for tumour infiltrative growth patterns”. In: *Journal of Theoretical Biology* 361 (2014), pp. 41–60. ISSN: 0022-5193.
- [4] A.K. Laird. “Dynamics of Tumor Growth”. In: *British Journal of Cancer* 13 (Sept. 1964), pp. 490–502.
- [5] W. V. Mayneord. “On a Law of Growth of Jensen’s Rat Sarcoma”. In: *The American Journal of Cancer* 16.4 (1932), pp. 841–846.
- [6] Franziska Michor et al. “What does physics have to do with cancer?” In: *Nature Reviews Cancer* 11.9 (2011), pp. 657–670. ISSN: 1474-1768.
- [7] HP Greenspan. “On the growth and stability of cell cultures and solid tumors”. In: *Journal of theoretical biology* 56.1 (1976), pp. 229–242.
- [8] J S Lowengrub et al. “Nonlinear modelling of cancer: bridging the gap between cells and tumours”. In: *Nonlinearity* 23.1 (Dec. 2009), R1–R91.
- [9] J Behrens et al. “Dissecting tumor cell invasion: epithelial cells acquire invasive properties after the loss of uvomorulin-mediated cell-cell adhesion”. In: *The Journal of cell biology* 108.6 (1989), pp. 2435–2447. ISSN: 1540-8140.
- [10] Allison L. Berrier and Kenneth M. Yamada. “Cell–matrix adhesion”. In: *Journal of Cellular Physiology* 213.3 (2007), pp. 565–573.
- [11] G Sciumè et al. “Tumor growth modeling from the perspective of multiphase porous media mechanics”. In: 3 (Sept. 2012), pp. 193–212.
- [12] G Sciumè et al. “Three phase flow dynamics in tumor growth”. In: *Computational Mechanics* 53.3 (2014), pp. 465–484.
- [13] Mauro Ferrari. “Problems in (nano)medical mechanics”. In: *International Journal of Non-Linear Mechanics* 56 (2013). Soft Matter: a nonlinear continuum mechanics perspective, pp. 3–19. ISSN: 0020-7462.
- [14] Robert M. Sutherland and Ralph E. Durand. “Hypoxic Cells in an in Vitro Tumour Model”. In: *International Journal of Radiation Biology and Related Studies in Physics, Chemistry and Medicine* 23.3 (1973), pp. 235–246.
- [15] D.L.S McElwain and L.E. Morris. “Apoptosis as a volume loss mechanism in mathematical models of solid tumor growth”. In: *Mathematical Biosciences* 39.1-2 (1978), pp. 147–157. ISSN: 0025-5564.
- [16] Judah Folkman and Mark Hochberg. “Self-regulation of growth in three dimensions”. In: *The Journal of experimental medicine* 138.4 (1973), pp. 745–753.
- [17] Robert M Sutherland, John A McCredie, and W Rodger Inch. “Growth of multicell spheroids in tissue culture as a model of nodular carcinomas”. In: *Journal of the National Cancer Institute* 46.1 (1971), pp. 113–120.
- [18] Gabriel Helmlinger et al. “Solid stress inhibits the growth of multicellular tumor spheroids”. In: *Nature biotechnology* 15.8 (1997), pp. 778–783.
- [19] Laura J Kaufman et al. “Glioma expansion in collagen I matrices: analyzing collagen concentration-dependent growth and motility patterns”. In: *Biophysical journal* 89.1 (2005), pp. 635–650.
- [20] Luigi Preziosi and Andrea Tosin. “Multiphase and multiscale trends in cancer modelling”. In: *Mathematical Modelling of Natural Phenomena* 4.3 (2009), pp. 1–11.

- [21] Mark AJ Chaplain, Luigi Graziano, and Luigi Preziosi. “Mathematical modelling of the loss of tissue compression responsiveness and its role in solid tumour development”. In: *Mathematical medicine and biology: a journal of the IMA* 23.3 (2006), pp. 197–229.
- [22] Leon Glass. “Instability and Mitotic Patterns in Tissue Growth”. In: *IFAC Proceedings Volumes* 6.4 (1973). IFAC Conference on Regulation and Control in Physiological Systems, Rochester, USA, 22-24 August, pp. 129–131. ISSN: 1474-6670.
- [23] John A. Adam. “A simplified mathematical model of tumor growth”. In: *Mathematical Biosciences* 81.2 (1986), pp. 229–244. ISSN: 0025-5564.
- [24] John A. Adam. “A mathematical model of tumor growth. II. effects of geometry and spatial nonuniformity on stability”. In: *Mathematical Biosciences* 86.2 (1987), pp. 183–211. ISSN: 0025-5564.
- [25] J.A. Adam and S.A. Maggelakis. “Mathematical models of tumor growth. IV. effects of a necrotic core”. In: *Mathematical Biosciences* 97.1 (1989), pp. 121–136. ISSN: 0025-5564.
- [26] Robert A. Gatenby and Edward T. Gawlinski. “A Reaction-Diffusion Model of Cancer Invasion”. In: *Cancer Research* 56.24 (1996), pp. 5745–5753. ISSN: 0008-5472.
- [27] Robert A. Gatenby. “Population Ecology Issues in Tumor Growth”. In: *Cancer Research* 51.10 (1991), pp. 2542–2547. ISSN: 0008-5472.
- [28] Robert A. Gatenby. “The Potential Role of Transformation-induced Metabolic Changes in Tumor-Host Interaction”. In: *Cancer Research* 55.18 (1995), pp. 4151–4156. ISSN: 0008-5472.
- [29] Heiko Enderling and Mark A.J. Chaplain. “Mathematical Modeling of Tumor Growth and Treatment”. In: *Current Pharmaceutical Design* 20.30 (2014), pp. 4934–4940. ISSN: 1381-6128/1873-4286.
- [30] A. R. A. Anderson et al. “Mathematical Modelling of Tumour Invasion and Metastasis”. In: *Journal of Theoretical Medicine* 2.2 (2000), pp. 129–154.
- [31] Alexander R. A. Anderson. “A hybrid mathematical model of solid tumour invasion: the importance of cell adhesion”. In: *Mathematical Medicine and Biology: A Journal of the IMA* 22.2 (2005), pp. 163–186. ISSN: 1477-8599.
- [32] A. Gerisch and M.A.J. Chaplain. “Mathematical modelling of cancer cell invasion of tissue: Local and non-local models and the effect of adhesion”. In: *Journal of Theoretical Biology* 250.4 (2008), pp. 684–704. ISSN: 0022-5193.
- [33] G Sciumè et al. “A multiphase model for three-dimensional tumor growth”. In: *New journal of physics* 15.1 (2013), p. 015005.
- [34] William G Gray and Cass T Miller. “Thermodynamically constrained averaging theory approach for modeling flow and transport phenomena in porous medium systems: 1. Motivation and overview”. In: *Advances in Water Resources* 28.2 (2005), pp. 161–180.
- [35] Helen Byrne and Luigi Preziosi. “Modelling solid tumour growth using the theory of mixtures”. In: *Mathematical medicine and biology : a journal of the IMA* 20 (Jan. 2004), pp. 341–66.
- [36] J. J. Casciari, S. V. Sotirchos, and R. M. Sutherland. “Mathematical modelling of microenvironment and growth in EMT6/Ro multicellular tumour spheroids”. In: *Cell Proliferation* 25.1 (1992), pp. 1–22.
- [37] Luigi Preziosi and Guido Vitale. “A multiphase model of tumor and tissue growth including cell adhesion and plastic reorganization”. In: *Mathematical Models and Methods in Applied Sciences* 21.09 (2011), pp. 1901–1932.
- [38] Tiina Roose, Stephen Chapman, and Philip Maini. “Mathematical Models of Avascular Tumor Growth”. In: *SIAM Rev* 49 (June 2007), pp. 179–208.
- [39] Steven M Wise et al. “Three-dimensional multispecies nonlinear tumor growth—I: model and numerical method”. In: *Journal of theoretical biology* 253.3 (2008), pp. 524–543.

- [40] Yangjin Kim, Magdalena A Stolarska, and Hans G Othmer. “The role of the microenvironment in tumor growth and invasion”. In: *Progress in biophysics and molecular biology* 106.2 (2011), pp. 353–379.
- [41] D Ambrosi, L Preziosi, and G Vitale. “The interplay between stress and growth in solid tumors”. In: *Mechanics Research Communications* 42 (2012), pp. 87–91.
- [42] M. S. Alnaes et al. “The FEniCS Project Version 1.5”. In: *Archive of Numerical Software* 3 (2015).
- [43] Robert C. Kirby and Anders Logg. “A compiler for variational forms”. In: *ACM Transactions on Mathematical Software* 32.3 (Sept. 2006), pp. 417–444. ISSN: 0098-3500.
- [44] Martin S. Alnaes et al. *Unified Form Language: A domain-specific language for weak formulations of partial differential equations*. 2012. arXiv: 1211.4047 [cs.MS].
- [45] Robert C. Kirby. “Algorithm 839: FIAT, a New Paradigm for Computing Finite Element Basis Functions”. In: *ACM Trans. Math. Softw.* 30.4 (Dec. 2004), pp. 502–516. ISSN: 0098-3500.
- [46] M.S. Alnaes et al. “Unified framework for finite element assembly”. In: *International Journal of Computational Science and Engineering* 4.4 (2009), pp. 231–244.
- [47] Anders Logg and Garth N. Wells. “DOLFIN”. In: *ACM Transactions on Mathematical Software* 37.2 (Apr. 2010), pp. 1–28. ISSN: 0098-3500.